Sensing and Bio-Sensing Research 25 (2019) 100292

Contents lists available at ScienceDirect

Sensing and Bio-Sensing Research

journal homepage: www.elsevier.com/locate/sbsr

Effect of tapering diameters with microbottle resonator for formaldehyde (CH_2O) liquid sensing

Md Ashadi Md Johari[a,b], Muhammad Imran Mustafa Abdul Khudus[c], Mohd Hafiz Bin Jali[a,d], M.S. Maslinda[a], Ummu Umairah Mohamad Ali[a], Sulaiman Wadi Harun[a], A.H. Zaidan[e], R. Apsari[e], M. Yasin[e,*]

[a] *Department of Electrical Engineering, Faculty of Engineering, University of Malaya, 50603 Kuala Lumpur, Malaysia*
[b] *Faculty of Engineering Technology, Universiti Teknikal Malaysia Melaka, 76100 Melaka, Malaysia*
[c] *Department of Physics, Faculty of Science, University of Malaya, 50603 Kuala Lumpur, Malaysia*
[d] *Faculty of Electrical Engineering, Universiti Teknikal Malaysia Melaka, 76100 Melaka, Malaysia*
[e] *Department of Physics, Faculty of Science and Technology, Airlangga University, Surabaya (60115), Indonesia*

ARTICLE INFO

Keywords:
Whispering gallery mode
Optical microbottle resonator
Tapered microfiber
Quality factor
Formaldehyde liquid

ABSTRACT

In this study, we demonstrate the effect of the microbottle resonator (MBR) based on whispering gallery modes (WGMs) with two different diameters of tapered microfibre and its experiment with the formaldehyde (CH_2O) liquid sensor. The MBR with the bottle diameter, D_b, of 190 *μm* was categorized by many spectra of transmission modes. Then, the MBR was energized through two tapered microfibres with different diameters, 8 *μm* and 10 *μm*. Differences between the two tapered microfibres with the MBR were determined for different concentration levels of sensing liquid. In addition, p-values and stability levels of the two tapered microfibres were calculated. According to the comparison results, the 8 *μm* tapered microfiber has a much better competency than the 10 *μm* tapered microfiber when using the MBR.

1. Introduction

Recently, the optical microresonator (OMR) has received considerable. By supporting the whispering gallery mode (WGM), it has gained a potential towards application in optical microsystems and miniaturization attention [1,2]. The microtoroid, microsphere and microdisc representing several geometries of the OMR allow coupling the lowest volume mode with the high quality factor (Q-factor) value [3]. The process is completed by having a total internal reflection between the formation of WGMs and the microcavity surrounding the medium. These microresonators are considered as 2-D resonators while confining the mode in equatorial planes and allowed spectral properties defined by their diameters.

OMRs supporting WGMs have been investigated to incorporate cylindrical shaped structures. For example, optical filaments and OMRs framed on strands are appraised for their particular way of confining light, easy handling and useful applications [4,5]. Another example includes the microbottle resonator (MBR) that has increased considerable attention because of its capability to support 3-D light confinement of the WGM through a combination of the WG-bouncing ball and WG-ring principle [6]. The area of the WGM confinement model can be defined with two distinctive MBR turning points corresponding to the regional field enhancement. The efficiency of the add/drop function can be increased owing to the presence of distinctive turning points in MBRs [7]. MBRs are able to generate complex spectra transmitted with high degenerated resonances, which is different with spherical microresonator structure [8]. This is possible owing to multiple overlapping MBR radii that allow bringing up the resonance spectra and trap the light close to the MBR surface [9].

Formaldehyde is a dull toxic gas blended by the oxidation of methanol and utilized as a germicide, disinfectant, histologic fixative and broadly useful substance reagent for research facility applications [10]. Formaldehyde promptly dissolves in water and generally disperses as a 37% arrangement in water. Formalin, which is a 10% arrangement of formaldehyde in water, is utilized as a disinfectant and for protecting organic examples. Formaldehyde can be found naturally in smoke from fires, car fumes and tobacco smoke. Small quantities of formaldehyde can be accumulated via typical metabolic processes in many life forms, including people [11]. It could cause throat, noise and eye irritation, breathing difficulties, coughing, nausea, severe vomiting, sneezing,

* Corresponding author.
E-mail address: yasin@fst.unair.c.id (M. Yasin).

https://doi.org/10.1016/j.sbsr.2019.100292
Received 23 April 2019; Received in revised form 12 June 2019; Accepted 2 July 2019

abdominal pain, renal injury, coma and fatality risk if consumed in a large amount [12]. Since formaldehyde has been established as best-known indoor air pollutant, effective and accurate formaldehyde detection need to be designed to reduce the detrimental effect on the human health. Thus, a simple, low cost and sensitive sensing approach is crucially important for formaldehyde detection. To date several sensing method to detect formaldehyde has been employed such as spectroscopy, cataluminense, chemiresistor, gas chromatography and high performance liquid chromatography (HPLC) [13–16]. However, most of these techniques have some drawbacks in term of cost, sensing time or complicated process.

Thus, in this paper, a simple sensing approach is proposed and demonstrated based on MBR. In this study, we conducted experiments with a formaldehyde (CH_2O) liquid sensor using an MBR with different tapering diameters, i.e., 8 µm and 10 µm. The MRB was formed using a procedure called 'soften-and-compressed', which creates a bottle structure from the standard SMF-28 fibre. The level of formaldehyde in the liquids used for this study was between 0% and 5%. The liquids were prepared by mixing formaldehyde with distilled water. The MBR was exposed to these liquids for the sensing purpose.

2. Experimental setup

The silica fibre was placed inside a splicing machine (Furukawa Electric Fitel S178A) with high temperatures being applied at the middle of the fibre while pressing both sides of the fibre at the same time. This arching process changed the structure of the silica fibre to make a bottle. The diameter of the bottle was determined by the number of bends . The MBR can be physically defined by the following three parameters: bottle distance across D_b, stem width D_s and neck-to-neck length L_b (Fig. 1). In this study, D_b was set to 190 µm. The fine tapering process was applied on the silica single mode fibre (SMF) to produce microfibre with two different diameters, 8 µm and 10 µm, which allowed a bundle of modes bouncing on the MBR surface and utilizing the WGM [17,18].

The tuneable laser source (ANDO AQ4321D) operating at wavelength range from 1520 nm to 1620 nm was utilized for MBR characterization on bare microfibres with different sizes, namely, 8 µm and 10 µm. The interval scale was 0.001 nm for the wavelength range between 1551.3 nm and 1551.6 nm for all concentration levels, while the output power value was measured using an optical power meter (THORLABS S145C).

Fig. 2(a) illustrates the sharp resonant depth of the transmitted spectra at various liquid concentrations of formaldehyde when the waist diameter of bare microfiber was fixed at 8 µm. In each stage of the concentration level, the insertion loss varies between −22 dBm and − 38 dBm, where its value was decreasing when concentration level was increasing [19]. The insertion loss was significantly different for every concentration level, which was influenced by the non-adiabatic microfibre and concentration of the liquid.

In Fig. 2 (b), the waist diameter of the bare microfibre used in the experiment is 10 µm. This value allowed to achieve sharp depth resonation of the transmission modes for every concentration level, which is similar to Fig. 2(a) . However, the insertion loss varies between −6.2 d Bm and − 9.4 dBm, which is much higher than the previous size of the bare microfibre. The insertion loss decreased with the increasing liquid concentration value. The size of the bare microfibre formed with the non-adiabatic structure considerably influenced the insertion loss.

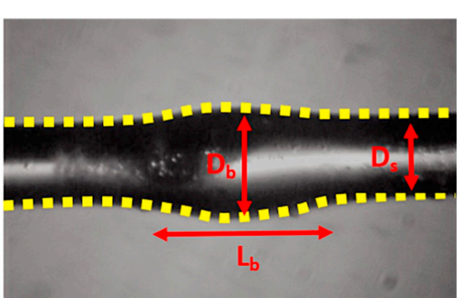

Fig. 1. SFM-25 structure changed to the microbottle resonator (MBR) with L_b = 182 µm, D_b = 190 µm and D_s = 125 µm after the arc procedure.

Fig. 3 illustrates the experimental setup for formaldehyde liquid concentration level sensing used for different bare microfibres. The MBR was placed between the bare microfibre and liquid surface, where the MBR at the bottom side was dipped into the liquid, while the top of the MBR was attached using the bare microfibre. The idea was to allow transmission of the spectra resonated on the MBR surface and experience the WGM with the formaldehyde molecule adsorbed along the MBR surface. The positions of the microfiber crossing and MBR surface immerse in formaldeyde solution are essential in ensuring that the optical properties of the WGM may be compared. Therefore, to ensure precision, we have controlled several parameters throughout the experiment by using a three-axis micro-positioning stage. The distance between the MBR and tapered fibre is fixed at 0 µm for all measurements and the cross position of the microfiber is position 90° perpendicular to the MBR. The position of formaldeyde liquid is at the centre of the MBR.

The optical power metre was connected to the end of the setup for the output data collection, while the tuneable laser source attached to the other end of the fibre supplied the light source. The concentration of formaldehyde varied from 0% to 5%. A wavelength of 1551.3 nm was used for every concentration level as transmitted power. The experiment was repeated three times to minimize the random error. The results were recorded for all conditions. For the stability testing, the transmission of spectra was recorded during 60 s for different concentrations. All tests were conducted on two different bare microfibers for the comparison purpose.

3. MBR performance as a CH_2O liquid sensor with different microfiber diameters

The average level of spectrum transmission using bare microfibres with diameters of 8 µm and 10 µm and the MBR with D_b = 190 µm for different concentration level is illustrated in Fig. 4. Both bare microfibres demonstrated a decreasing trend as the concentration level of liquid increased, with the 8 µm microfibre showing a more steep slope than that of the 10 µm microfibre. As mentioned in Table 1, the 8 µm tapered microfibre showed a better performance for all tested parameters in terms of linearity, sensitivity, standard deviation and p-value. The MBR with the 8 µm bare microfibre achieved 3.6251 dBm/%, which is higher than that of the MBR with the 10 µm bare microfibre achieving only 0.278 dBm/%. The linearity of the MBR with the 8 μm bare microfibre was over 95%, while for the other setup it was less than 60%. Overall, the MBR with the 8 µm bare microfibre achieves a better result than the MBR with the 10 µm bare microfibre. However, the losses were higher for the 10 μm bare microfibre compared to that of the 8 µm bare microfibre. This is because the tapering waist diameters were different, which led to more losses for every concentration level tested [20–22].

The sensing performance depends on the accuracy of the collected data. Hence, the experiment was repeated three times for all conditions, which also reduced the random error that probably happened during the experiment [23]. The results are shown in Fig. 5, where the three experiments are represented by the three line graphs for both the 8 µm and 10 µm bare microfibres used with the MBR. Notably, when comparing Fig. 5(a) and Fig. 5(b), the 8 µm bare microfibre demonstrates a fine decreasing line as opposed to that of the 10 µm bare microfibre. This fine line somehow influenced the analysis of the bare microfibres on their sensing performance and capability. The 8 µm bare microfibre

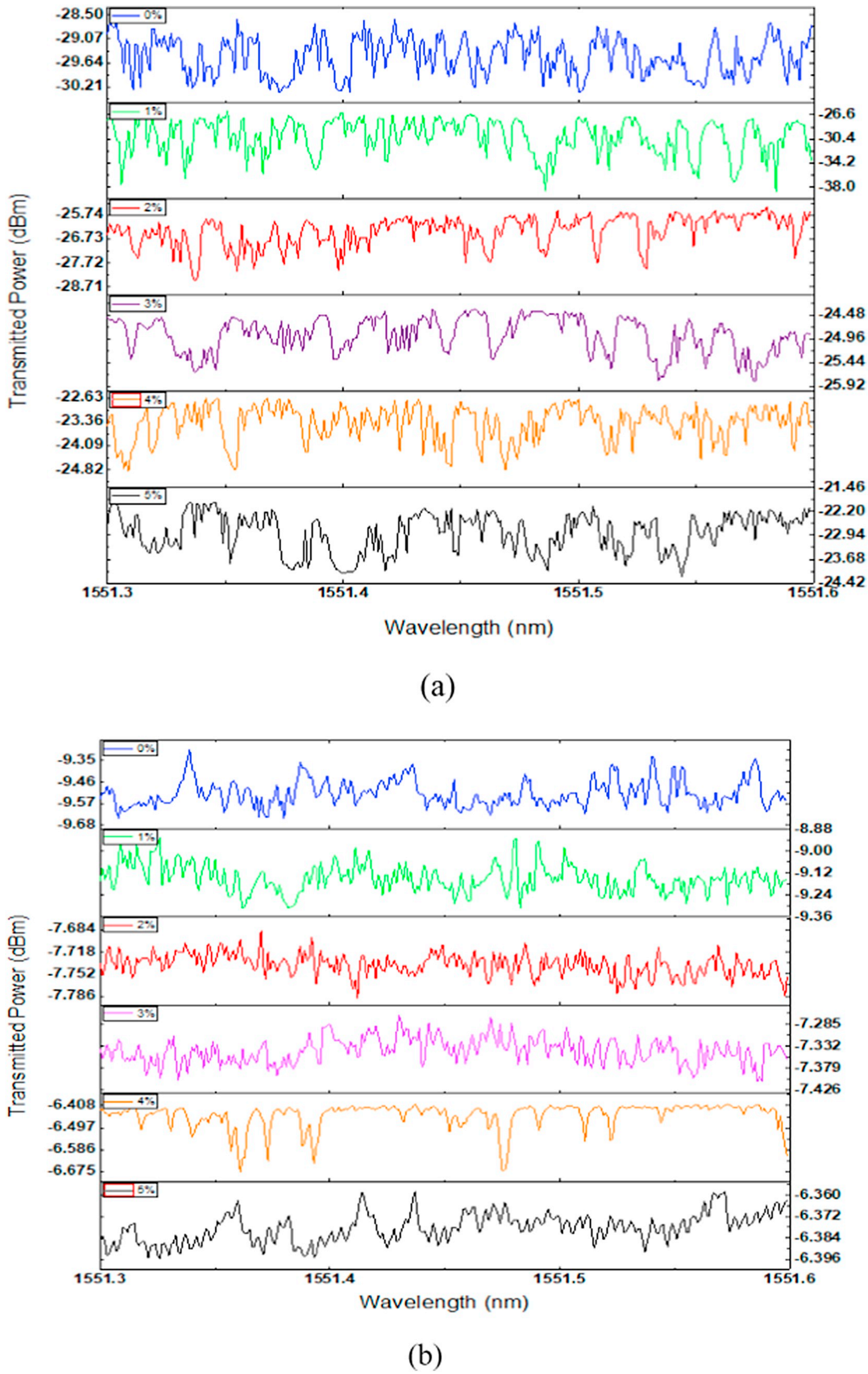

Fig. 2. The MBR transmission spectra for different concentration levels:
(a) 8 μm tapered fibre waist diameter and (b) 10 μm tapered fibre waist diameter.

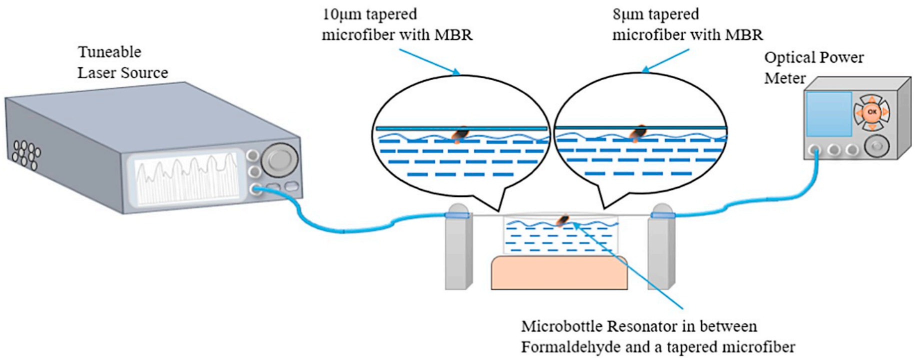

Fig. 3. MBR with formaldehyde and bare microfibres with the waist diameter of 8 μm and 10 μm for concentration liquid sensing.

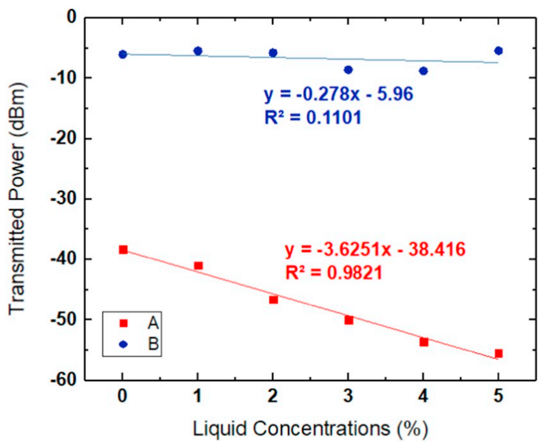

Fig. 4. Transmitted power values for different concentration levels of formaldehyde for the MBR with 8 μm bare microfibre (A) and 10 μm bare microfibre (B).

Table 1
Performance analysis of the 8 μm and 10 μm bare microfibres with the MBR in formaldehyde sensing.

Parameters	8 μm Bare microfibre	10 μm Bare microfibre
Linearity (%)	99.10%	33.18%
Sensitivity (dBm/% concentration)	3.6251	0.278
Standard deviation (dBm)	1.497	6.365
P-value	8.3×10^{-7}	7.59×10^{-5}
Linear range (%)	0–5	0–5

with the MBR showed stable results across the three experiments.

Fig. 6(a) and Fig. 6(b) represent the stability test for the 8 μm and 10 μm bare microfibres with the MBR performed for liquid concentration sensing during 60 s. The MBR with the 8 μm bare microfibre showed less stable results compared to that of the 10 μm bare microfibre. Hence, it can be concluded that the diameter of the bare microfibre influences the stability of sensing performance. Herein, the MBR with the 10 μm bare microfibre demonstrated more stable reactions for the different concentration levels than that with 8 μm. This is attributed to the handling of the microfiber, which is easier with a larger diameter and thus reduces the measurement errors.

Future work should be focused on exploring another sensing approach for the WGM sensor since the intensity based sensor may not produce an accurate measurement. The arrangement and structure of MBR and microfiber should be optimized to obtain a sharp resonance and the shift of resonance wavelength should be observed during changes in the environment or formaldehyde concentration.

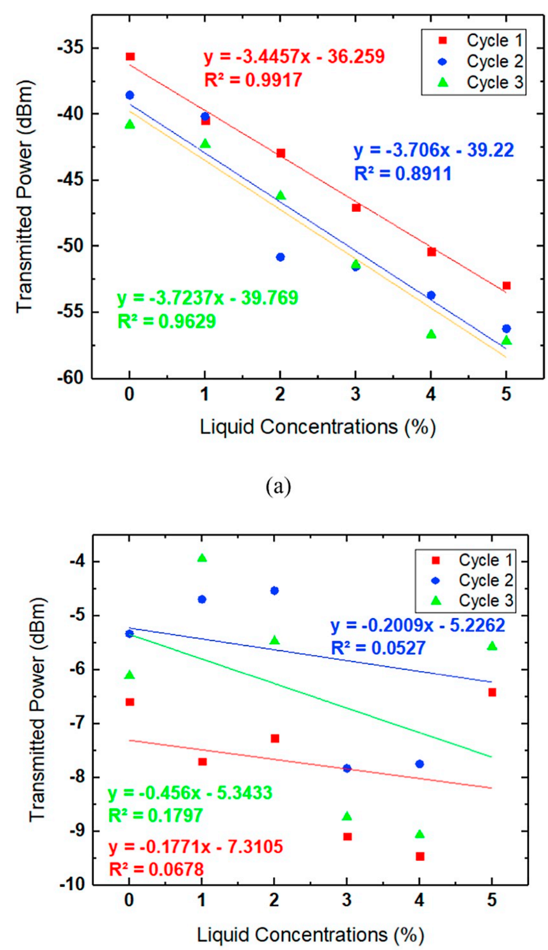

Fig. 5. Transmitted power value of (a) 8 μm and (b) 10 μm bare microfibre with the MBR for the three experiments with varied liquid concentration levels.

4. Conclusion

This paper described the performance of two microfibres with different diameters and the MBR utilized as a formaldehyde liquid sensor. A method known as 'soften-and-compressed' was applied to a silica fibre that created a bulge area on the fibre called the MBR with the stem diameter of 125 μm, bottle diameter of 190 μm and bottle length of 182 μm. The MBR was then excited through the two tapered microfibres with the diameters of 8 μm and 10 μm via a tuneable laser source and characterized by shifting the wavelength of the TLS from 1551.30 *nm* to

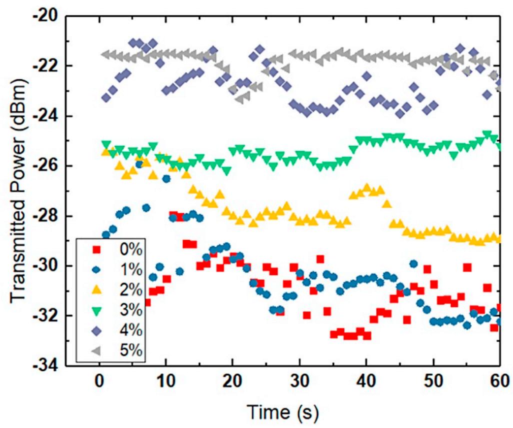

(a)

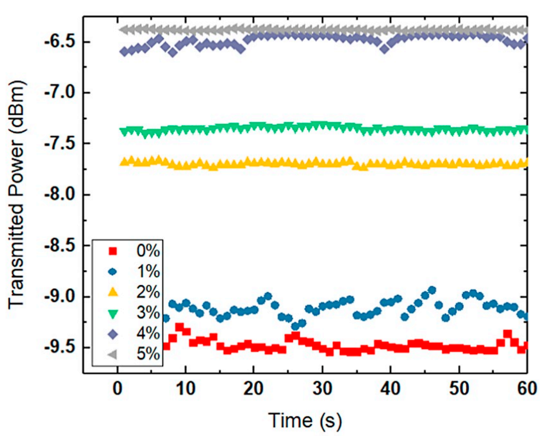

(b)

Fig. 6. Transmitted power of (a) 8 μm and (b) 10 μm bare microfibre with the MBR for stability performance with 60 s of data collection.

1551.60 *nm* with the wavelength interval of 0.001 *nm*. The comparison between the two different diameters of the tapered fibre was reported based on four parameters: linearity, sensitivity, standard deviation and p-value. According to the results, the 8 μm tapered microfibre is more efficient than the one with the waist diameter of 10 μm. The p-values for each dimeter was $> 10^{-5}$, while the stability of the two tapered microfibres was measured during 60 s.

Acknowledgments

The authors would like to acknowledge Indonesia Government through World Class Research Grant (2019) and Airlangga University, Indonesia. This work also was supported by University of Malaya, Faculty of Engineering Technology, Universiti Teknikal Malaysia Melaka and Ministry of Education, Malaysia for their financial support.

References

[1] K.J. Vahala, Optical microcavities, Nature 424 (6950) (2003) 839.
[2] A.B. Matsko, V.S. Ilchenko, Optical resonators with whispering gallery modes I: basics, IEEE J. Sel. Top. Quantum Electron 12 (3) (2006) 3.
[3] M. Sumetsky, Y. Dulashko, R. Windeler, Optical microbubble resonator, Opt. Lett. 35 (7) (2010) 898–900.
[4] V.S. Ilchenko, et al., Microtorus: a high-finesse microcavity with whispering-gallery modes, Opt. Lett. 26 (5) (2001) 256–258.
[5] M. Sumetsky, Whispering-gallery-bottle microcavities: the three-dimensional etalon, Opt. Lett. 29 (1) (2004) 8–10.
[6] G.S. Murugan, J.S. Wilkinson, M.N. Zervas, Optical excitation and probing of whispering gallery modes in bottle microresonators: potential for all-fiber add–drop filters, Opt. Lett. 35 (11) (2010) 1893–1895.
[7] G.S. Murugan, J.S. Wilkinson, M.N. Zervas, Selective excitation of whispering gallery modes in a novel bottle microresonator, Opt. Express 17 (14) (2009) 11916–11925.
[8] M. Sumetsky, et al., Surface nanoscale axial photonics: robust fabrication of high-quality-factor microresonators, Opt. Lett. 36 (24) (2011) 4824–4826.
[9] G.S. Murugan, et al., Hollow-bottle optical microresonators, Opt. Express 19 (21) (2011) 20773–20784.
[10] T. Salthammer, S. Mentese, R. Marutzky, Formaldehyde in the indoor environment, Chem. Rev. 110 (2010) 2536–2572.
[11] P.-R. Chung, C.-T. Tzeng, M.-T. Ke, C.-Y. Lee, Formaldehyde gas sensors: a review, Sensors 13 (2013) 4468–4484.
[12] R. Golden, Identifying an indoor air exposure limit for formaldehyde considering both irritation and cancer hazards, Crit. Rev. Toxicol. 41 (2011) 672–721.
[13] F. Bianchi, M. Careri, M. Musci, A. Mangia, Fish and food safety: determination of formaldehyde in 12 fish species by SPME extraction and GC–MS analysis, Food Chem. 100 (2007) 1049–1053.
[14] X. Weng, C.H. Chon, H. Jiang, D. Li, Rapid detection of formaldehyde concentration in food on a polydimethylsiloxane (PDMS) microfluidic chip, Food Chem. 114 (2009) 1079–1082.
[15] L. Aksornneam, P. Kanatharana, P. Thavarungkul, C. Thammakhet, 5-Aminofluorescein doped polyvinyl alcohol film for the detection of formaldehyde in vegetables and seafood, Anal. Methods 8 (2016) 1249–1256.
[16] P.E. Georghiou, C.K. Ho, The chemistry of the chromotropic acid method for the analysis of formaldehyde, Can. J. Chem. 67 (1989) 871–876.
[17] K. Lim, et al., Fabrication and applications of microfiber, Selected Topics On Optical Fiber Technology, InTech, 2012.
[18] M.N.M. Nasir, G.S. Murugan, M.N. Zervas, Spectral cleaning and output modal transformations in whispering-gallery-mode microresonators, JOSA B 33 (9) (2016) 1963–1970.
[19] Y. Zhao, Z. Deng, Q. Wang, Fiber optic SPR sensor for liquid concentration measurement, Sensors Actuators B Chem. 192 (2014) 229–233.
[20] S. Khaliq, S.W. James, R.P. Tatam, Fiber-optic liquid-level sensor using a long-period grating, Opt. Lett. 26 (16) (2001) 1224–1226.
[21] F.J. Arregui, et al., Optical fiber humidity sensor using a nano Fabry–Perot cavity formed by the ionic self-assembly method, Sensors Actuators B Chem. 59 (1) (1999) 54–59.
[22] N.M. Isa, et al., Polyaniline doped poly (methyl methacrylate) microfiber for methanol sensing, IEEE Sensors J. 18 (7) (2018) 2801–2806.
[23] H. Ohno, et al., Industrial applications of the BOTDR optical fiber strain sensor, Opt. Fiber Technol. 7 (1) (2001) 45–64.